

The following resources related to this article are available online at <http://stke.sciencemag.org>.
This information is current as of 29 May 2010.

Article Tools	Visit the online version of this article to access the personalization and article tools: http://stke.sciencemag.org/cgi/content/full/sigtrans;3/120/ra35
Supplemental Materials	"Supplementary Materials" http://stke.sciencemag.org/cgi/content/full/sigtrans;3/120/ra35/DC1
Related Content	The editors suggest related resources on <i>Science's</i> sites: http://stke.sciencemag.org/cgi/content/abstract/sigtrans;3/121/pc10
References	This article has been cited by 1 article(s) hosted by HighWire Press; see: http://stke.sciencemag.org/cgi/content/full/sigtrans;3/120/ra35#BIBL This article cites 39 articles, 11 of which can be accessed for free: http://stke.sciencemag.org/cgi/content/full/sigtrans;3/120/ra35#otherarticles
Glossary	Look up definitions for abbreviations and terms found in this article: http://stke.sciencemag.org/glossary/
Permissions	Obtain information about reproducing this article: http://www.sciencemag.org/about/permissions.dtl

In Vivo Identification of Regulators of Cell Invasion Across Basement Membranes

David Q. Matus,¹ Xiao-Yan Li,^{2,3} Sarah Durbin,¹ Daniel Agarwal,^{1*} Qiuyi Chi,¹ Stephen J. Weiss,^{2,3} David R. Sherwood^{1†}

(Published 4 May 2010; Volume 3 Issue 120 ra35)

Cell invasion through basement membranes during development, immune surveillance, and metastasis remains poorly understood. To gain further insight into this key cellular behavior, we performed an *in vivo* screen for regulators of cell invasion through basement membranes, using the simple model of *Caenorhabditis elegans* anchor cell invasion, and identified 99 genes that promote invasion, including the genes encoding the chaperonin complex *cct*. Notably, most of these genes have not been previously implicated in invasive cell behavior. We characterized members of the *cct* complex and 11 other gene products, determining the distinct aspects of the invasive cascade that they regulate, including formation of a specialized invasive cell membrane and its ability to breach the basement membrane. RNA interference-mediated knockdown of the human orthologs of *cct-5* and *lit-1*, which had not previously been implicated in cell invasion, reduced the invasiveness of metastatic carcinoma cells, suggesting that a conserved genetic program underlies cell invasion. These results increase our understanding of the genetic underpinnings of cell invasion and also provide new potential therapeutic targets to limit this behavior.

INTRODUCTION

The ability of cells to traverse the barriers imposed by the basement membrane (BM), the dense sheet-like extracellular matrix that surrounds most tissues, is a critical cellular behavior that occurs during both normal ontogeny and immune system function (1). For example, trophoblast cells breach the endometrium BM to establish the placenta (2), and leukocytes cross the perivascular BM to reach sites of infection and injury (3). Uncontrolled invasive cell activity is also associated with various human diseases, most notably cancer, where transformed cells are thought to hijack developmental invasive programs to metastasize (4, 5). Despite its importance in both development and human disease, cell invasion through the BM remains poorly understood (1, 3, 6–8). Most of the work on cell invasion has been limited to *in vitro* models, which do not reflect the *in vivo* microenvironment and endogenous BM architecture (9, 10). Although recent advances in imaging technology are providing new insights into cell invasion in vertebrates (11), it remains challenging to perform functional perturbations in these models and simultaneously visualize the complex, dynamic process of cell invasion through BMs.

Anchor cell (AC) invasion in *C. elegans* is a simple model of cell invasion through BMs that combines forward genetics with single-cell visual analysis. During *C. elegans* larval development, the AC, a specialized gonadal cell, breaches the gonadal and ventral epidermal BMs to contact the central primary-fated vulval precursor cells (1° VPCs), initiating uterine-vulval connection (12, 13). AC invasion is a regulated and robust process, which occurs invariantly before the P6.p four-cell stage in wild-type animals (Fig. 1A) (12). During the L2-L3 molt (approximately

6 hours before invasion), a specialized invasive cell membrane, rich in F-actin and actin regulators, is established in the AC through coordination of netrin (14) and integrin (15) signaling at the interface of the AC and BM (Fig. 1A). AC invasion is stimulated by an unidentified chemotactic cue secreted by the underlying 1° VPCs (Fig. 1A). The ability of the AC to breach the underlying BMs in response to this cue is dependent on two oncogenes, the bZIP transcription factor (TF) *fos-1a* (13) and zinc finger TF, *egl-43L*, the *C. elegans* ortholog of vertebrate EVI1 and MEL paralogs (16, 17). Together, these TFs regulate the expression of the zinc metalloproteinase *zmp-1* as well as other targets encoding pro-invasive factors in the AC (13).

Toward the goal of comprehensively identifying regulators of cell invasion through the BM *in vivo*, we have performed a focused whole-genome RNA interference (RNAi) screen. Here, we report the identification of 99 regulators of AC invasion, most of which have not been previously implicated in invasion or metastasis. We have further characterized the genes encoding the most robust pro-invasive factors, including members of the *cct* complex and 11 others, encompassing both known oncogenes and previously unknown regulators of cell invasion. Notably, small interfering RNA (siRNA)-mediated knockdown of two of these pro-invasive genes reduced the invasiveness of metastatic carcinoma cells, suggesting that our approach has identified conserved regulators that might be potential therapeutic targets in halting cancer progression.

RESULTS

An RNAi screen identifies 99 regulators of AC invasion

A defect in AC invasion disrupts uterine-vulval attachment and results in an easily observed Protruded vulva (Pvl) and Egg-laying defective (Egl) phenotype. We have taken advantage of data collected from a number of whole-genome RNAi screens that have identified the complement of genes giving a Pvl or Egl phenotype after RNAi depletion (18–20). Using these data, we examined 539 genes that produce a Pvl or Egl phenotype

¹Biology Department, Duke University, Durham, NC 27708, USA. ²Division of Molecular Medicine and Genetics, Department of Internal Medicine, University of Michigan, Ann Arbor, MI 48109, USA. ³Life Sciences Institute, University of Michigan, Ann Arbor, MI 48109, USA.

*Present address: Weill Cornell Medical College, 1300 York Avenue, New York, NY 10065, USA.

†To whom correspondence should be addressed. E-mail: david.sherwood@duke.edu

after RNAi knockdown, using Nomarski optics at the time of AC invasion (table S1). We identified 99 genes whose reduction results in a failure of the AC to breach the BM, as evidenced by an unbroken phase-dense line underneath the AC (Fig. 1B and tables S2 and S3). Ninety-five percent (94 of 99) of these genes have human orthologs as determined by BLASTP analysis, of which 90% (85 of 94 genes) have not been previously implicated in cell invasion or cancer metastasis (table S2). Validating the specificity and rigor of this approach, we identified components of genetic pathways known to promote AC invasion, including the TFs *fos-1a* (13) and *egl-43L* (16, 17); the netrin receptor *unc-40* (14); and the integrin α subunit *ina-1* (15) (Table 1 and table S2).

Eleven pro-invasive genes and the *cct* complex regulate the AC's ability to breach the BM

To focus on the most crucial regulators of AC invasion, we further characterized genes whose RNAi depletion gave a robust AC invasion defect, which we set at >30%, a degree of penetrance similar to invasion defects resulting from RNAi directed against members of known AC invasion pathways, including FOS-1A and EGL-43L activity, as well as INA-1 and UNC-40 signaling (Table 1 and tables S2 and S3). This list includes genes with human orthologs that have been implicated directly in cell

invasion and metastasis [*hda-1*, a histone deacetylase (21), and *cdc-37*, a co-chaperone of hsp90 (22)], as well as previously unknown regulators (*mep-1*, C48A7.2, *cacn-1*, F28F8.5, T20B12.1, *lit-1*, T03F1.8, *hbl-1*, *unc-62*, and the *cct* complex) (Table 1). The genes whose RNAi knockdown gave the most robust AC invasion defect (>79%) included seven of the eight-member *cct* chaperonin complex (Table 1 and tables S2 and S3). Because AC invasion defects were similar for all *cct* genes tested (Table 1 and table S2), we further characterized several members of this complex, *cct-2*, *cct-5*, *cct-6*, and *cct-7* (henceforth referred to as *cct*). Consistent with our RNAi results, AC invasion defects were detected in putative null alleles for *mep-1*, *hda-1*, C48A7.2, and *cct-6* (table S4 and fig. S1). For genes lacking putative null alleles or whose loss of function prevented animals from surviving to the time of AC invasion, we observed AC invasion defects by using multiple double-stranded RNA (dsRNA) constructs, ruling out off-target RNAi effects (23) (table S4). To verify that the observed AC invasion defect was specifically because of failure to breach the underlying BM, we examined the integrity of laminin, a key structural component of BM. After RNAi depletion targeting *cct* and the remaining 11 genes, LAM-1::GFP (laminin) remained intact under the AC after a failure to invade, confirming that the invasion defects were due to an inability to break through the BM (Fig. 1B and fig. S2).

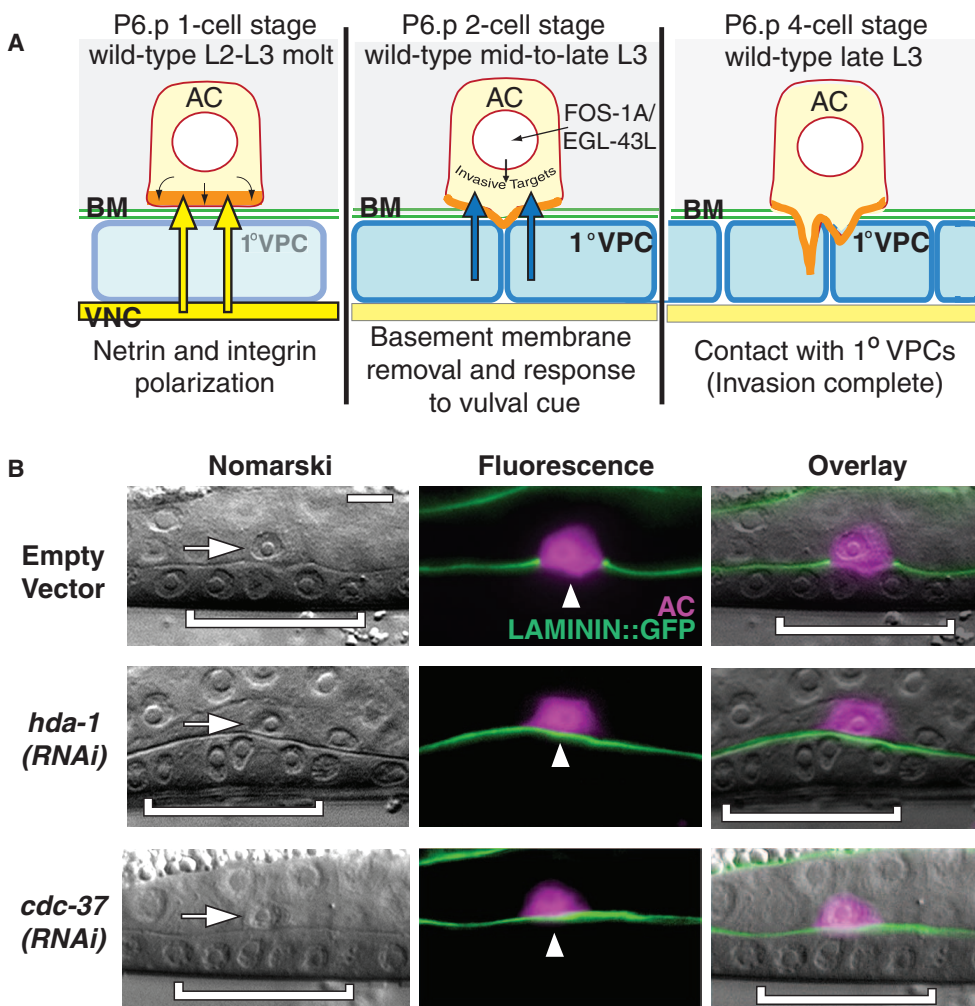


Fig. 1. Summary of *C. elegans* AC invasion and invasion defects after RNAi depletion. **(A)** Schematic representation of the known mechanisms underlying AC invasion. At the L2-L3 molt (P6.p one-cell stage; left), approximately 6 hours before invasion, UNC-6 (netrin) secretion (yellow arrows) from the ventral nerve cord (VNC) and integrin signaling polarize the AC's basal cell membrane by recruiting F-actin, actin regulators, and the netrin receptor (UNC-40; orange) toward the juxtaposed BMs (shown in green) (14, 15). During the mid-to-late L3 stage (P6.p two-cell stage; middle), an unidentified cue from the 1° VPCs (blue arrows) stimulates invasive protrusions from the AC that require the activity of the TFs FOS-1A and EGL-43L to breach the BM. During the late L3 stage (P6.p four-cell stage), the AC contacts the P6.p granddaughters, initiating the connection between the developing uterine and the vulval epithelium. **(B)** Nomarski image (left), corresponding fluorescence image (middle), and overlay (right). Anterior is left and ventral is down. In wild-type or worms fed control RNAi (L4440 empty vector; top panel), the AC (magenta, *zmp-1::mCherry*; white arrowhead) breaches the BM (green, LAM-1::GFP) and contacts the central primary fated P6.p granddaughters (bracket; P6.p four-cell stage). In contrast, after RNAi-mediated knockdown of *hda-1* and *cdc-37* (middle and bottom panels, respectively), the BMs remain intact after a failure in AC invasion (table S3). Scale bar, 5 μ m.

Invasion is promoted by nine genes and the *cct* complex, which function in the AC after specification

To understand how these newly identified genes regulate invasion, we first examined transcriptional and translational green fluorescent protein (GFP) reporters for localization and abundance. We found that the *cct* complex and six other genes—*mep-1*, a zinc finger TF; *lit-1*, an ortholog

of NEMO-like kinase (NLK); *cdc-37*; T03F1.8, a guanylate kinase; and two uncharacterized conserved proteins, *cacn-1* and T20B12.1—were up-regulated in the AC before or during the time of invasion (Fig. 2, A to G, and figs. S3 and S4), similar to other known regulators of AC invasion [such as *fos-1a*, *zmp-1*, *egl-43L*, and *pat-3* (the integrin β subunit)] (*13, 15–17*). Additionally, we identified three genes—*hda-1*; F28F8.5,

Table 1. A subset of genes for which RNAi depletion inhibits AC invasion. Genes in bold are known regulators of cell invasion or metastasis. Genes marked with an asterisk have been previously implicated in AC invasion. A dagger (†) denotes members of the *cct* complex selected for

further characterization. AC invasion defect is listed as the percent average defect from multiple trials (minimum of two) at the P6.p 4-cell stage of 1° VPC division. See tables S2 and S3 for a complete list of pro-invasive genes and the penetrance of their AC invasion defect by RNAi.

Gene public name (reference)	Sequence name (gene)	CDS description	Homolog BLASTP e-value	Homologous protein	Homolog description	AC invasion defect (%)
<i>Transcription factors</i>						
<i>hbl-1</i>	F13D11.2	C2H2-type zinc finger	1.10E-20	ENSEMBL: ENSP00000340749	Isoform 2 of zinc finger protein 124	42
*<i>fos-1a</i> (13, 28)	F29G9.4	BZIP transcription factor	0.000000017	VG:OTTHUMP0000200848	FOS-like antigen 2	45
<i>mep-1</i>	M04B2.1	Zinc finger protein				45
<i>unc-62</i>	T28F12.2	Homeodomain transcription factor	7.10E-79	ENSEMBL: ENSP00000326296	Isoform Meis2C of homeobox protein Meis2	35
*<i>egl-43L</i> (16, 17, 29)	R53.3	Zinc finger, C2H2 type (four domains)	9.10E-47	ENSEMBL: ENSP00000367643	PRDM16 (EVI1/MEL)	33
<i>Chromatin remodeling and architecture</i>						
<i>hda-1</i> (21, 32)	C53A5.3	Yeast RPD3 protein like	2.80E-170	ENSEMBL: ENSP00000362649	Histone deacetylase 1	57
<i>Protein synthesis, degradation, and folding</i>						
<i>cct-1</i>	T05C12.7	TCP-1-like chaperonin	3.70E-196	ENSEMBL: ENSP00000317334	T-complex protein 1 subunit α	88
<i>fcct-2</i>	T21B10.7	TCP-1-like chaperonin	5.11E-183	ENSEMBL: ENSP00000299300	T-complex protein 1 subunit β	80
<i>cct-4</i>	K01C8.10	TCP-1-like chaperonin	4.30E-179	ENSEMBL: ENSP00000377958	T-complex protein 1 subunit δ	81
<i>fcct-5</i>	C07G2.3	TCP-1-like chaperonin	1.90E-203	ENSEMBL: ENSP00000280326	T-complex protein 1 subunit ϵ	86
<i>fcct-6</i>	F01F1.8	TCP-1-like chaperonin	8.39E-183	ENSEMBL: ENSP00000275603	T-complex protein 1 subunit ζ	79
<i>fcct-7</i>	T10B5.5	TCP-1-like chaperonin	7.10E-188	ENSEMBL: ENSP00000258091	T-complex protein 1 subunit η	83
<i>cct-8</i>	Y55F3AR.3	TCP-1-like chaperonin	3.60E-166	ENSEMBL: ENSP00000286788	T-complex protein 1 subunit θ	81
<i>cdc-37</i> (22, 33)	W08F4.8	Hsp90 co-chaperone	2.00E-73	ENSEMBL: ENSP00000222005	Hsp90 co-chaperone Cdc37	44
<i>Signaling and membrane trafficking</i>						
*<i>ina-1</i> (15, 31)	F54G8.3	Integrin α chain	2.00E-83	ENSEMBL: ENSP00000264107	Isoform α -6X1A of integrin α -6 precursor	30
*<i>unc-40</i> (14, 30)	T19B4.7	Membrane protein	1.30E-164	ENSEMBL: ENSP00000304146	Netrin receptor DCC precursor	58
<i>lit-1</i>	W06F12.1	Serine-threonine kinase (CDC2/CDC28 subfamily)	2.50E-144	ENSEMBL: ENSP00000262393	Nemo-like kinase	31
<i>Metabolism</i>						
<i>T03F1.8</i>	T03F1.8	Guanylate kinase	1.30E-51	ENSEMBL: ENSP00000317659	Guanylate kinase	41
<i>C48A7.2</i>	C48A7.2	Phosphate permease	1.90E-105	ENSEMBL: ENSP00000272542	Sodium-dependent phosphate transporter 1	59
<i>Nematode-specific gene with unknown function</i>						
<i>F28F8.5</i>	F28F8.5					30
<i>Uncharacterized conserved genes</i>						
<i>T20B12.1</i>	T20B12.1		1.30E-90	ENSEMBL: ENSP00000313953	Tetratricopeptide repeat domain 27	45
<i>cacn-1</i>	W03H9.4		4.10E-112	ENSEMBL: ENSP00000221899	Isoform 2 of uncharacterized protein C19orf29	32

an uncharacterized nematode-specific gene; and C48A7.2, a sodium and phosphate transporter—which were expressed in most cells, including the AC (Fig. 2, H to J, and figs. S3 and S4). *hbl-1* and *unc-62* (the *C. elegans* orthologs of the TFs *hunchback* and *homothorax*, respectively) were not detected in the AC before or during the time of invasion, but were expressed in the underlying vulval cells (*unc-62>GFP*) or in the ventral nerve cord and underlying vulval cells at earlier stages of devel-

opment (*hbl-1::GFP*) (Fig. 2, K and L, and fig. S5). The absence of localization in the AC and expression in the vulval cells suggested that *hbl-1* and *unc-62* might act in VPCs to promote invasion. A summary of the localization of the proteins encoded by newly identified pro-invasive genes is shown in Fig. 2M.

AC invasion relies on the proper specification of the AC and the underlying 1° VPCs, which generate the invasive cue (12). To determine

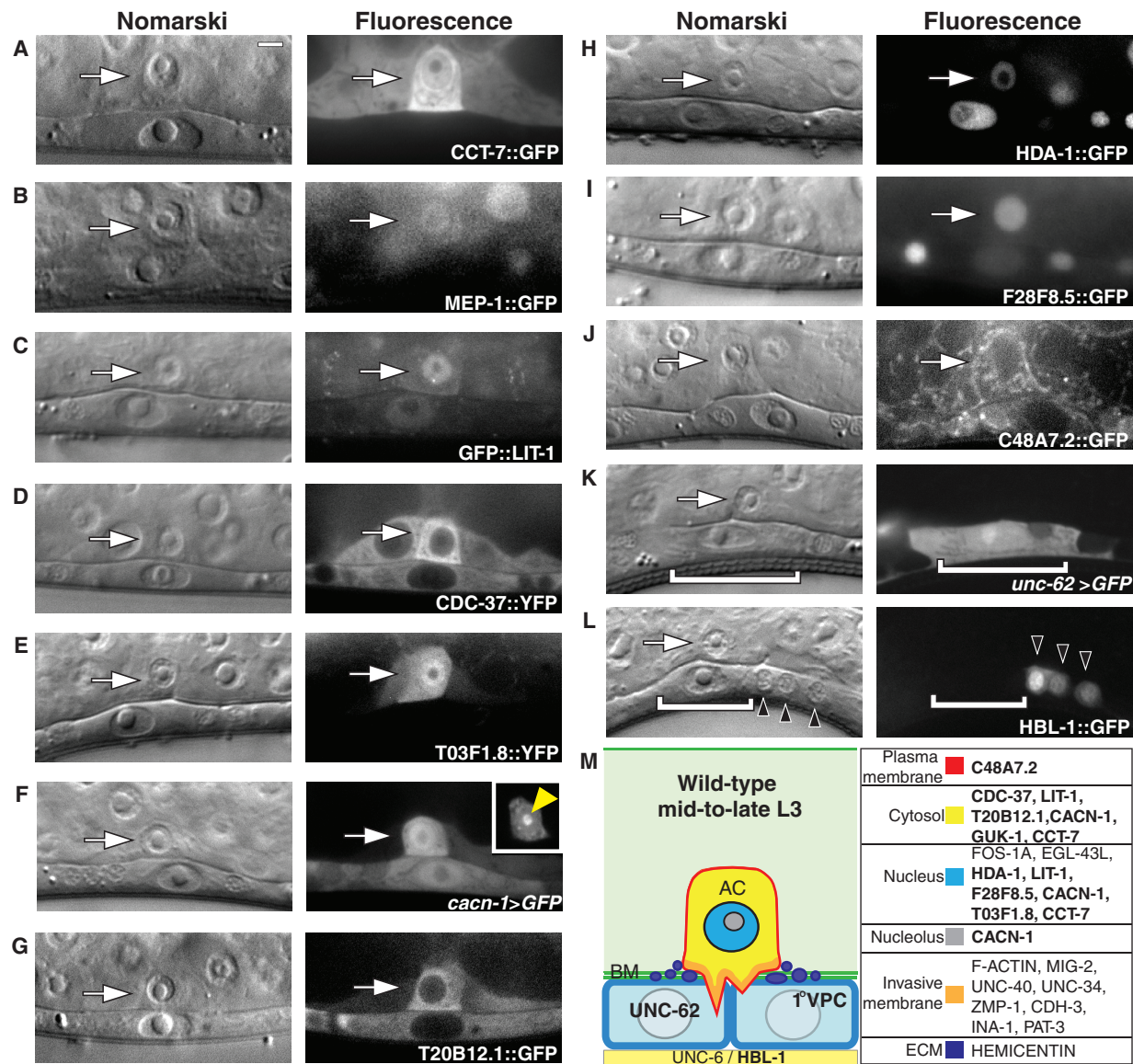


Fig. 2. Transgene reporter localization of newly identified genes that regulate AC invasion. Nomarski image, left; corresponding fluorescence image, right, at the P6.p one-cell stage. Anterior is left and ventral is down. All images are confocal z slices except (C) and (D), which are wide-field fluorescence images. (A to J) Translational (::) and transcriptional (>) reporter constructs for the *cct* complex (as shown by *cct-7::GFP*) and 9 of the 11 newly identified pro-invasive genes showed AC-enriched (arrow) GFP localization in various subcellular compartments before and during AC invasion. (K) A transcriptional reporter for *unc-62* (*unc-*

62>GFP) showed VPC expression before and during the time of AC invasion (white brackets). (L) A translational reporter for *HBL-1* (*hbl-1::GFP*) was detected in the cell bodies of the ventral nerve cord (black arrowheads) before and during the time of AC invasion. Although *HBL-1::GFP* is not localized to the VPCs at the time of invasion, it is expressed in VPCs hours before invasion (fig. S5). (M) Summary diagram of the sub-cellular localization of proteins in the AC, underlying 1° VPCs, and VNC during invasion. Genes identified in this study are bolded. Scale bar, 5 μm.

whether these newly identified genes regulate invasion by causing defects in AC or 1° VPC cell specification, we examined the expression of *lin-3>GFP* and *egl-17>GFP*, markers of AC and 1° VPC cell fate, respectively (24, 25). *lin-3>GFP* was detected in the AC after RNAi-mediated depletion of the *cct* complex and the remaining 11 genes, indicating that AC

specification was normal despite reduction of activity of these genes (fig. S6). The expression of *egl-17>GFP* in the underlying vulval cells was lost only after depletion of *unc-62* by RNAi, consistent with a role for *unc-62* in regulating invasion by controlling 1° VPC specification (fig. S7). Additionally, RNAi knockdown of *hbl-1* resulted in precocious

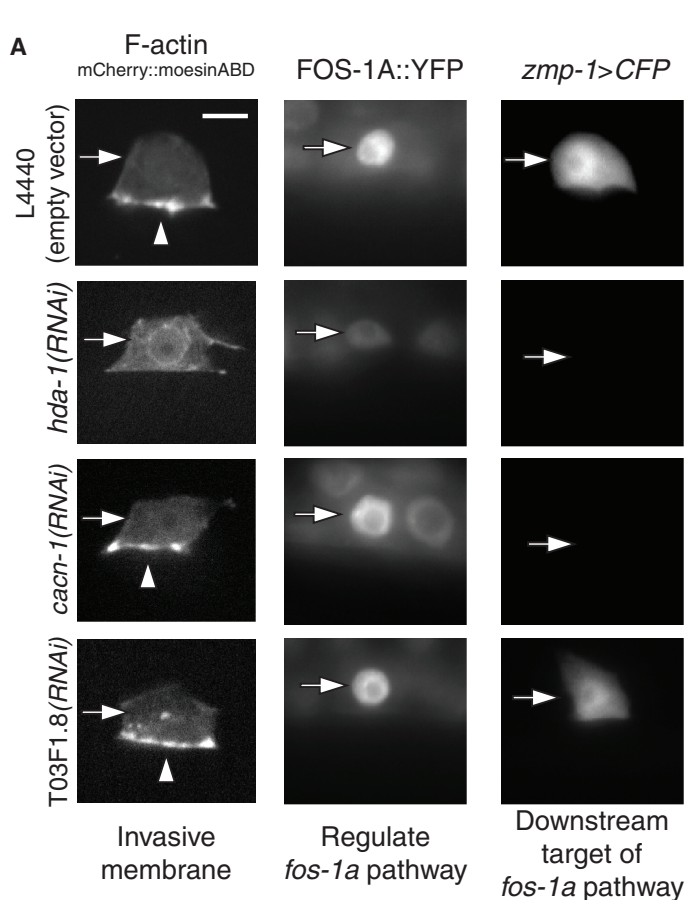
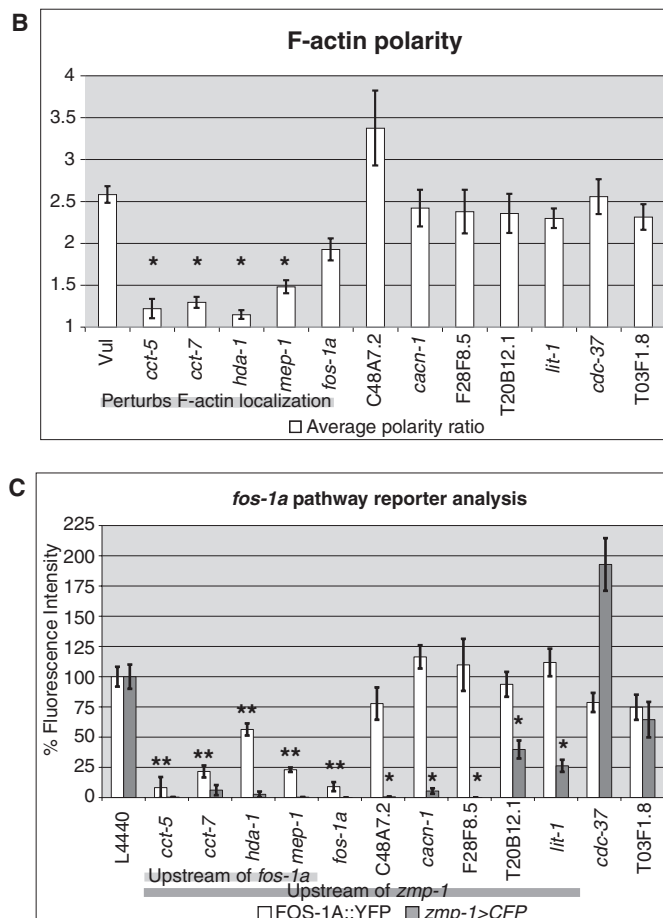


Fig. 3. Newly identified regulators of AC invasion function within established as well as previously uncharacterized pathways to promote invasion. **(A)** Confocal z slice fluorescence images of F-actin probe (left; mCherry::moeABD) and wide-field fluorescence images of FOS-1A::YFP (middle) and *zmp-1>CFP* (right) in empty vector control and *hda-1*, *cacn-1*, and T03F1.8 RNAi-depleted animals at the time of invasion. A single-factor ANOVA followed by Tukey's post hoc test for significance was used in all cases. For this and all subsequent figures, *n* refers to the number of animals per genotype. The top panel shows localization or expression for all three reporters in wild-type ACs. RNAi depletion of *hda-1* resulted in a loss of F-actin at the invasive membrane ($n = 18$; $P < 0.05$) and reduced FOS-1A::YFP fluorescence in the AC ($n > 10$; $P > 0.05$). *zmp-1>CFP* expression was significantly reduced after RNAi depletion of *hda-1* or *cacn-1* ($n = 12$ for both; $P < 0.05$), but not of T03F1.8 ($n = 10$; $P > 0.05$). **(B and C)** Quantification of an F-actin probe (B) and FOS-1A::YFP/*zmp-1>CFP* (C) in



Vulvaless (Vul), empty vector control (L4440), and RNAi-depleted animals in which the AC failed to invade ($n > 10$ animals for each RNAi depletion). * $P < 0.05$. **(B)** RNAi depletion of the *cct* complex, *hda-1*, and *mep-1* blocked polarization of F-actin at the invasive membrane (gray bar). In Vul animals, AC invasion is blocked, but polarity is maintained (14). Knockdown of the other genes caused defects in AC invasion, although the ACs were still polarized. Loss of C48A7.2 resulted in reduced AC size, which could account for an F-actin polarity ratio that is greater than in Vul control animals. **(C)** RNAi knockdown of the *cct* complex, *hda-1*, and *mep-1* decreased the expression of FOS-1A::YFP ($P < 0.05$; white bars) and its downstream target, *zmp-1>CFP* ($P < 0.05$; black bars) in the AC (denoted by the double asterisks). RNAi targeting five genes (C48A7.2, *cacn-1*, F28F8.5, T20B12.1, and *lit-1*) reduced *zmp-1>CFP* expression in the AC ($P < 0.05$), but did not affect FOS-1A::YFP expression (denoted by the single asterisk). *cdc-37* and T03F1.8 RNAi depletion did not significantly decrease the expression of either *fos-1a* pathway reporter ($P > 0.05$). Although *cdc-37(RNAi)* increased *zmp-1>CFP* expression, we have previously shown that increased *zmp-1* expression does not alter invasion (13). Error bars report the SEM. Scale bar, 5 μ m.

egl-17>GFP expression and division of the VPCs (figs. S5B and S7), a heterochronic phenotype that leads to inability of the AC to respond to the early release of the vulval cue (12). Together with the transgene localization of *unc-62>GFP* and *hbl-1::GFP*, these results suggest that *unc-62* and *hbl-1* promote AC invasion by regulating 1° VPC specification, and that the remaining nine pro-invasive genes and *cct* complex appear to influence postspecification aspects of the invasive process.

To further examine the function of this subset of genes from our screen that promote invasion, we used a *C. elegans* strain in which only uterine tissue, including the AC, is sensitive to RNAi (15) (table S5). RNAi depletions targeting *cct* and nine other genes, all of which showed transgene localization in the AC (Fig. 2, A to J), blocked invasion (table S5). Because uterine cells do not contribute to AC invasion (12), an AC invasion defect in this background indicates that the gene functions in the AC. In contrast, RNAi targeting *hbl-1* and *unc-62*, which were not expressed in the AC (Fig. 2, K and L) showed normal invasion in the uterine-specific RNAi-sensitive background (table S5), consistent with the data above suggesting that these genes function within the vulval cells. We conclude that most of the genes identified in our screen that block invasion after reduction of activity function within the AC.

Genes that function within the AC regulate multiple aspects of invasion

Before invasion, netrin and integrin signaling in the AC establish a specialized F-actin-rich invasive cell membrane that contacts the underlying

BM (14, 15). To determine whether any of the pro-invasive genes that function in the AC regulate the formation of this invasive cell membrane domain, we used a probe containing the F-actin-binding domain of the moesin gene (mCherry::moeABD) to visualize F-actin at the invasive membrane (14). RNAi targeting *cct*, *hda-1*, or *mep-1* resulted in loss of polarized F-actin, indicating a failure to form the invasive cell membrane (Fig. 3, A and B, and fig. S8). Consistent with this finding, both the *cct* complex (26) and the histone deacetylases (HDACs) (21, 27) regulate the actin cytoskeleton and cell motility in mammalian cells. To determine whether these four genes regulate invasive membrane formation through interactions with netrin or integrin signaling, we examined the localization of the netrin receptor (UNC-40::GFP) and integrin β subunit PAT-3 (PAT-3::GFP) after RNAi knockdown. Localization of the netrin receptor (fig. S9) or of integrin (fig. S10) at the invasive membrane was not altered after reduction of *cct*, *hda-1*, or *mep-1*, which suggests that these genes function independently of netrin and integrin receptor localization to regulate the polarization of the F-actin cytoskeleton.

Independent of invasive membrane formation, the ability of the AC to breach the underlying BM relies on at least two TFs, *fos-1a* and *egl-43L*, which function in the AC to regulate the expression of downstream targets, including the zinc metalloproteinase *zmp-1* (13, 16, 17). To determine whether any of the genes functioning within the AC regulate the *fos-1a-egl-43L* pathway, we quantified the fluorescence of a translational reporter for *fos-1a* (*fos-1a::YFP*) and a transcriptional reporter for *zmp-1* (*zmp-1>CFP*). Loss of five of the genes (C48A7.2, *cacn-1*, F28F8.5,

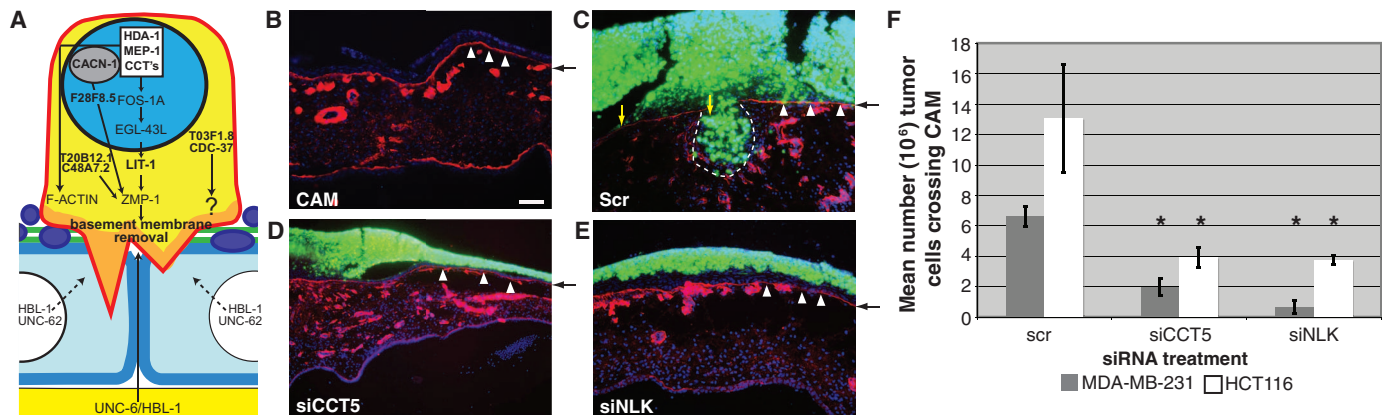


Fig. 4. Identification of conserved regulators of cell invasion through BM. (A) Newly identified AC invasion-promoting genes were mapped onto preexisting molecular pathways governing AC invasion. Two TFs, *hbl-1* and *unc-62*, appear to indirectly affect invasion by regulating 1° VPC specification. Upstream regulators (*hda-1*, *mep-1*, and the *cct* complex; black box) control both the establishment of the AC invasive membrane and the *fos-1a* transcriptional pathway underlying BM removal. Additionally, genes were identified that function within (*lit-1*) and parallel to (*cacn-1*, F28F8.5, T20B12.1, C48A7.2) the *fos-1a* pathway. Lastly, we have identified two genes, *cdc-37* and T03F1.8, that act in distinct aspects of AC invasion beyond the establishment of the invasive membrane and *fos-1a* pathway. (B to F) CCT5 and NLK are required for tissue-invasive activity of breast and colon tumor cells in vivo. GFP-labeled MDA-MB-231 cells were transfected with a control siRNA (SCR) or siRNA directed against CCT5 (siCCT5) or NLK (siNLK). The transfectants were cultured for 3 days on top of the CAM of 11-day-old chicks. Chick BM and cell nuclei in cross sections were visualized by staining with an antibody

directed against type IV collagen (red) and with 4,6-diamidino-2-phenylindole (DAPI; blue), respectively. (B) Cross section of chick CAM in the absence of overlying cancer cells shows the ectodermal BM (white arrowheads) at the CAM surface (position indicated by the black arrow). Vascular structures, which are surrounded by type IV collagen, can also be observed along with the endodermal BM along the lower edge of the CAM. (C) GFP-labeled MDA-MB-231 cells electroporated with scrambled siRNA (Scr) breach the chick BM. Invading cancer cells are outlined with white dashed lines. Areas of BM degradation are demarcated with yellow arrows. White arrowheads mark areas with intact BM. (D and E) MDA-MB-231 cells electroporated with siRNAs directed against CCT5 or NLK fail to breach the BM. (F) Invasion is quantified as the number of breast (MDA-MB-231) and colon (HCT116) tumor cells (10⁶) that cross the CAM surface (mean invasion \pm SEM of three or more experiments) after siRNA knockdown of CCT5 and NLK (**P* < 0.001) relative to control (Scr) siRNA treatment, using a single-factor ANOVA followed by Tukey's post hoc test for significance. Scale bar, 100 μ m.

T20B12.1, and *lit-1*) reduced the expression of *zmp-1>CFP*, but not the abundance of FOS-1A::YFP, and loss of two genes (*cdc-37* and T03F1.8) did not decrease the expression of either reporter (Fig. 3, A and C, and figs. S11 and S12). RNAi depletion of *cct*, *hda-1*, and *mep-1* decreased both FOS-1A::YFP abundance and *zmp-1>CFP* expression. These results suggest that HDACs may play a conserved role in the transcriptional regulation of *fos* family oncogenes during invasion, because in mammalian cell culture, HDAC inhibition represses invasion in *v-fos* transformed cells and leads to the reexpression of normally suppressed genes (21). Notably, loss of the *cct* genes, *hda-1*, and *mep-1* also perturbed F-actin polarity, revealing a set of upstream regulators that control both *fos-1a*-dependent BM removal and invasive membrane formation (13–15).

Of the five genes that promoted *zmp-1>CFP* expression, only the abundance of the translational reporter for *lit-1* (*GFP::lit-1*) was decreased by *fos-1* RNAi depletion, indicating that *lit-1* is a target of *fos-1a* (figs. S13 and S14A). Additionally, *lit-1* RNAi depletion did not affect FOS-1A::YFP abundance or *egl-43L>GFP* expression in the AC (fig. S14), which suggests that it acts downstream of *fos-1a* and *egl-43L* but upstream of *zmp-1* to promote AC invasion (Fig. 4A). The remaining four genes that promote *zmp-1>CFP* expression appear to act parallel to the *fos-1a* pathway, because *fos-1* RNAi depletions did not affect the abundance of their reporters (fig. S13). Together, these experiments identify three main groups of genes that promote AC invasion: (i) upstream regulators controlling both the establishment of the invasive membrane and BM removal through the *fos-1a* pathway (*cct* complex members, *mep-1*, and *hda-1*); (ii) genes that are downstream (*lit-1*) or parallel (C48A7.2, F28F8.5, T20B12.1, and *cacn-1*) to the *fos-1a* pathway; and (iii) two genes (*cdc-37* and T03F1.8) that fail to regulate either invasive membrane formation or components of the *fos-1a* pathway, which suggests that they control distinct aspects of AC invasion (Fig. 4A).

***cct-5/CCT5* and *lit-1/NLK* are required for invasion in carcinoma cells**

The human orthologs of genes that promote AC invasion [*fos-1a*/FOS family members (28), *egl-43L/EVI-1* (29), netrin (30), and integrin (31)] regulate the tissue-invasive activity of mammalian cells. Similarly, several of the human orthologs to genes identified in our screen have been directly implicated in controlling cell invasion or metastasis, including *HDA1* and *CDC37*, both of which are targets of anticancer therapeutics (32, 33). To determine whether any of the other newly identified genes also regulate the invasive behavior of mammalian cells, we used siRNA to knock down human orthologs of two genes, *cct-5/CCT5* and *lit-1/NLK*, in transformed human breast cancer cells (MDA-MB-231) and colon carcinoma cells (HCT116) explanted onto a chick chorioallantoic membrane (CAM), an *ex vivo* system used to assay the ability of cells to cross an endogenous BM (34) (Fig. 4B). Although not linked previously to tissue-invasive activity, members of the CCT–TCP-1 complex are thought to function as chaperones for various proteins, including actin and tubulin monomers (26), and NLK is a negative regulator of the canonical Wnt signaling pathway (35). After electroporation with scrambled siRNA controls, breast and colon carcinoma cells could breach the BM of the chick CAM (Fig. 4C). Strikingly, siRNA-mediated knockdown of either CCT5 or NLK reduced invasion in both cancer cell lines, leaving the BM intact under the proliferating tumor mass (Fig. 4, D and E, and fig. S15, B and C). siRNA-mediated depletion of CCT5 and NLK did not significantly affect breast carcinoma cell proliferation, migration, or apoptosis (fig. S15, E and F), suggesting that these genes specifically affect the BM transmigration activity of the cancer cells. Together, these results suggest that the genes identified that control AC invasion might also be components of a conserved mechanism used by mammalian cells to breach BM barriers.

DISCUSSION

BM invasion is a critical process that occurs during development, immune system surveillance, and the spread of metastatic cancer. Here, we report the identification of 99 genes that promote AC invasion during *C. elegans* larval development through a loss-of-function screen to identify cell invasion regulators *in vivo*. We have identified genes with increased expression in the AC (*cdc-37* and *lit-1*), as well as several that were ubiquitously expressed (*hda-1*, F28F8.5, and C48A7.2), critically important genes that might be missed in expression-based studies to identify genes that regulate invasion. Remarkably, 90% of the pro-invasive genes that have human orthologs have not been previously implicated in cell invasion or cancer metastasis. We further characterized the most robust regulators of AC invasion, identifying *lit-1* as a new member of the *fos-1a* pathway, as well as a set of genes (*cct* complex, *hda-1*, and *mep-1*) that function to regulate multiple aspects of invasion, including the establishment of a specialized invasive membrane (14, 15) and the ability to remove underlying BM (13).

The basement membrane, which is an interwoven network of extracellular matrix molecules, is an ancient metazoan structure underlying the basal surface of epithelia and endothelia. The predominant components of the BM that provide structural support and barrier function are the meshwork of type IV collagen and laminin, which are evolutionarily conserved from sponges to humans (8, 36). Similar to other cell biological processes (such as stem cell determination and maintenance, apoptosis, regulation of cell division, and epithelial-to-mesenchymal transition), it has been suggested that the genetic networks controlling cell invasion during development are also conserved and redeployed during tumor invasion (1, 8, 34, 36, 37). Here, we provide additional evidence for the conservation of cell invasion programs during development and disease showing that the human orthologs of several newly identified regulators of AC invasion, including the genes encoding the *cct* complex and *lit-1*, which encodes an intracellular kinase, also function during carcinoma cell invasion. This suggests that much of the required invasion machinery is shared and that the regulators of cell invasion identified here might offer potent new therapeutic targets to modulate invasive cell behavior in development and human diseases such as cancer.

MATERIALS AND METHODS

Worm handling and strains

Wild-type nematodes were strain N2. Strains were reared at 15°, 20°, and 25°C under standard conditions (38). In the text and figures, we designate linkage to a promoter with the (>) symbol and linkages that fuse open reading frames with the (::) annotation (14). Vulvaless animals were created with the strain *lin-3(n1059)/lin-3(n378)* (12). The following transgenes and alleles were used for experiments performed in this paper: *qyIs42[pat-3::GFP, ina-1]*, *qyIs49[T03F1.8::YFP]*, *qyIs67[cdh-3>unc-40::GFP]*, *qyIs68[cdh-3>unc-40::GFP]*, *qyIs69[C48A7.2::YFP]*, *qyIs72[cdc-37::YFP]*, *qyIs91[egl-43L::GFP]*, *qyIs93[hda-1::GFP]*, *qyIs96[cacn-1>GFP]*, *qyIs99[unc-62>GFP]*, *qyIs100[T20B12.1::GFP]*, *qyIs102[fos-1a>rde-1]*, *qyIs114[cdh-3>cacn-1::GFP]*, *qyEx171[cct-7::GFP]*, *UL906[F28F8.5::GFP]*, *sEx10433[cct-2>GFP]*, *sEx12510[cct-7>GFP]*, *ctIs39[hbl-1::GFP]*, *neEx1[lit-1::GFP]*, *cgc5338Is1mep-1::GFP*; LGI: *ayIs4[egl-17>GFP]*, *dpy-5(e907)*; LGII: *cacn-1(tm3042)*, *cacn-1(tm3126)*, *cct-2(ok3438)*, *qyIs17[zmp-1>mCherry]*, *rrf-3(pk1426)*, *rol-6(n1270)*; LGIII: *cct-6(ok2904)*, *lit-1(ok649)*, *unc-119(ed4)*, *syIs107[lin-3>GFP]*; LGIV: *eri-1(mg366)*, *mep-1(n3702)*, *mep-1(q660)*, *mep-1(ok421)*, *syIs68[zmp-1>CFP]*, *dpy-20(e1282)*, *lin-3(n1059)/lin-3(n378)*; LGV: *hda-1(e1795)*, *hda-1(ok1595)*, *rde-1(ne219)*, *qyIs50[cdh-3>mCherry::moeABD]*;

LGX: *hbl-1(mg285)*, *hbl-1(ve18)*, *lin-15B(n744)*, *syIs123[fos-1a::YFP]*, *qyIs66[cdh-3>unc-40::GFP]*, *qyIs7[lam-1::GFP]*.

Molecular biology and generation of transgenic animals

Translational reporter constructs fusing coding sequences for GFP to complementary DNAs (cDNAs) encoding UNC-40, laminin, and the actin-binding domain of moesin have been described previously (14, 15). We used polymerase chain reaction (PCR) fusion (13) to generate *promoter>GFP* and *PROTEIN::GFP* constructs to the genes listed in table S6. AC-specific promoter fusions were generated with the *cdh-3^{mk62-63}* AC-specific regulatory element (13). Templates and specific primer sets for each promoter and reporter gene are listed in table S7. Transgenic worms were created by transformation with co-injection markers pPDM016B (*unc-119+*) into the germline of *unc-119(ed4)* worms. These expression constructs were injected with Eco RI-digested salmon sperm DNA and pBSSK-DNA at 50 to 100 ng/μl serving as carrier DNA along with serial dilutions of the GFP fusion construct to optimize expression levels and avoid toxicity. Transgenic extrachromosomal (Ex) lines and integrated strains (Is) generated in this study are listed in table S6. Integrated strains were generated as described previously (13).

RNA interference

dsRNA for the 539 genes listed in table S1 was delivered by feeding to *rrf-3(pk1426)* worms by means of the RNAi protocol that was originally used to produce a Pvl or Egl phenotype (L4 or L1 plating) (18–20). RNAi vectors from the Simmer *et al.* (18) and Rual *et al.* (20) dsRNA libraries were sequenced to verify the correct insert. One hundred-base pair dsRNA constructs were designed and cloned into L4440 to minimize any potential off-target RNAi affects with the Web portal dsCheck (<http://dscheck.mai.jp/>) (table S4) and fed to *rrf-3(pk1426)*; *lam-1::GFP* worms to verify AC invasion defects. Uterine-specific RNAi sensitivity was generated by restoring RDE-1 protein to the cells of the somatic gonad under the control of the *fos-1a* promoter in *rde-1(ne219)* mutant animals, using *rde-1(ne219)*; *fos-1a>rde-1*; *rrf-3(pk1426)* worms (15).

Image acquisition, processing, and analyses

Images were acquired by means of a Zeiss Axiolmager A1 microscope with a 100× plan-apochromat objective and a Zeiss AxioCam MRm charge-coupled device camera, controlled by Zeiss Axiovision software (Zeiss Microimaging), or with a Yokogawa spinning disk confocal mounted on a Zeiss Axiolmager A1 microscope using IVision software (Biovision Technologies). Images were processed in ImageJ (NIH Image) and overlaid with Photoshop CS3 (Adobe Systems).

AC invasion scoring, polarity, and fluorescence intensity measurements

AC invasion was evaluated in relation to the timing of P6.p descendant divisions, the L3 molt, gonad reflection, and ventral uterine (VU) cell divisions (13). For the initial RNAi screen, all 539 genes (table S1) targeted by feeding RNAi were scored with Nomarski optics for AC invasion defects and the production of adult Pvl and Egl phenotypes to confirm the effectiveness of the RNAi clone used. At least two independent dsRNA feeding experiments were performed for those genes that showed an AC invasion defect (defined as a minimum of two out of nine animals having a block in AC invasion) upon RNAi depletion (tables S2 and S3). Polarity measurements and ratios for F-actin (mCherry::moeABD) and UNC-40::GFP in wild-type, mutant, and RNAi-targeted strains were determined with ImageJ (NIH Image) v1.4 by comparing the average fluorescence intensity from five-pixel-wide line scans drawn along the invasive and noninvasive membranes of mCherry::moeABD and UNC-40::GFP in

wild-type and RNAi-depleted animals. A polarity ratio was generated by dividing the fluorescence density of the invasive membrane by the fluorescence density of the noninvasive membrane ($n > 10$ animals were scored for each genotype with an observable defect in AC invasion at the P6.p four-cell stage) (14, 15). Fluorescence intensity measurements of AC GFP abundance for translational reporters *fos-1a::YFP* (*syIs123*), *T20B12.1::GFP* (*qyIs100*), *GFP::lit-1* (*neEx1*), *F28F8.5::GFP* (*UL906*), *cdc-37::YFP* (*qyIs72*), and *T03F1.8::YFP* (*qyIs49*) and AC GFP expression of transcriptional reporters *zmp-1>CFP* (*qyIs17*), *egl-43L>GFP* (*qyIs91*), *cacn-1>GFP* (*qyIs96*) were determined with ImageJ (NIH Image) v1.4 (15) ($n > 10$ animals for each with an observable defect in AC invasion). In all cases, except quantification of GFP::LIT-1 abundance (by an unpaired Student's *t* test), a single-factor analysis of variance (ANOVA), followed by Tukey's post hoc test was used to determine statistical significance of changes in GFP abundance or polarity.

Tissue culture, siRNA electroporation, and CAM invasion assay

Human breast cancer cells (MDA-MB-231) or colon cancer cells (HCT116), marked with GFP, were grown in Dulbecco's modified Eagle's medium (DMEM) with 10% fetal bovine serum (FBS). Cells were transfected with 50 pmol each of control, CCT5, or NLK siRNA (Invitrogen) by electroporation with Amaxa Cell Line Nucleofector Kit V according to the manufacturer's instructions (Lonza). Silencing efficiency was established 48 hours after electroporation by reverse transcription PCR (RT-PCR) (fig. S15A). Transfected cells ($\sim 1 \times 10^6$) were cultured atop the CAM of 11-day-old chicken embryos for 3 days as described previously (34, 39). Invasion was monitored in cross sections of the fixed CAM by fluorescent microscopy with BM integrity assessed with a chick-specific mouse monoclonal antibody directed against type IV collagen (provided by J. Fitch and T. Linsenmayer, Tufts University). Invasion is expressed as the mean number of tumor cells (10^6) below the CAM surface; statistical significance was calculated by a single-factor ANOVA followed by Tukey's post hoc test. CAM invasion results obtained with a pool of CCT5 siRNAs or a single NLK siRNA were confirmed with at least two individual CCT5 siRNAs or a second independent siRNA directed against NLK (fig. S15B). Cancer cell migration, proliferation, and apoptosis (fig. S15, E and F) were quantified as described (34, 39).

SUPPLEMENTARY MATERIALS

www.sciencesignaling.org/cgi/content/full/3/120/ra35/DC1

Fig. S1. Putative null alleles of *mep-1*, *hda-1*, *cct-6*, *C48A7.2*, and *hbl-1* show AC invasion defects.

Fig. S2. LAM-1::GFP (laminin) is intact following RNAi targeting the *cct* complex and 11 other pro-invasive genes at the P6.p 4-cell stage of VPC division.

Fig. S3. Transgene reporter localization of newly identified pro-invasive genes at the P6.p 2-cell stage of VPC division.

Fig. S4. Transgene reporter localization of newly identified pro-invasive genes at the P6.p 4-cell stage of VPC division.

Fig. S5. *hbl-1* functions in VPC specification to promote AC invasion.

Fig. S6. The AC is correctly specified, as shown by *lin-3>GFP*, following RNAi depletion of the newly identified regulators of AC invasion.

Fig. S7. 1° VPC specification following RNAi depletion of newly identified AC invasion genes.

Fig. S8. Identification of regulators of invasive membrane formation.

Fig. S9. Regulators of invasive membrane formation function independently of netrin receptor localization.

Fig. S10. Regulators of invasive membrane formation function independently of integrin receptor localization.

Fig. S11. Identification of regulators of the *fos-1a* pathway.

Fig. S12. Identification of genes that act within or parallel to the *fos-1a* pathway.

Fig. S13. *fos-1a* RNAi depletion identifies *lit-1* as a new member of the *fos-1a* pathway.

Fig. S14. *lit-1* functions downstream of *fos-1a* and *egl-43L* during AC invasion.

Fig. S15. CCT5 and NLK siRNA-mediated knockdown specifically affect BM transmigration activity.

Table S1. 539 Pvl and Egl genes targeted by RNAi for AC invasion defects.

Table S2. Identification of 99 regulators of AC invasion.

Table S3. RNAi depletion of 99 genes results in an AC invasion defect.

Table S4. Timing and degree of AC invasion into the vulval epithelium: mutant analysis and off-target RNAi controls.

Table S5. Timing and degree of AC invasion into the vulval epithelium: uterine-specific RNAi.

Table S6. Extrachromosomal array and integrated strain generation.

Table S7. Primer sequences and templates used for PCR fusions and restriction enzyme cloning.

REFERENCES AND NOTES

1. R. G. Rowe, S. J. Weiss, Breaching the basement membrane: Who, when and how? *Trends Cell Biol.* **18**, 560–574 (2008).
2. P. Duc-Goiran, T. M. Mignot, C. Bourgeois, F. Ferré, Embryo-maternal interactions at the implantation site: A delicate equilibrium. *Eur. J. Obstet. Gynecol. Reprod. Biol.* **83**, 85–100 (1999).
3. R. Yadav, K. Y. Larbi, R. E. Young, S. Nourshargh, Migration of leukocytes through the vessel wall and beyond. *Thromb. Haemost.* **90**, 598–606 (2003).
4. M. R. Stratton, P. J. Campbell, P. A. Futreal, The cancer genome. *Nature* **458**, 719–724 (2009).
5. G. P. Gupta, J. Massagué, Cancer metastasis: Building a framework. *Cell* **127**, 679–695 (2006).
6. B. Podbilewicz, How does a cell anchor and invade an organ? *Dev. Cell* **5**, 5–7 (2003).
7. D. Hanahan, R. A. Weinberg, The hallmarks of cancer. *Cell* **100**, 57–70 (2000).
8. A. Srivastava, J. C. Pastor-Pareja, T. Igaki, R. Pagliarini, T. Xu, Basement membrane remodeling is essential for *Drosophila* disc eversion and tumor invasion. *Proc. Natl. Acad. Sci. U.S.A.* **104**, 2721–2726 (2007).
9. S. Even-Ram, K. M. Yamada, Cell migration in 3D matrix. *Curr. Opin. Cell Biol.* **17**, 524–532 (2005).
10. F. Sabeh, R. Shimizu-Hirota, S. J. Weiss, Protease-dependent versus -independent cancer cell invasion programs: Three-dimensional amoeboid movement revisited. *J. Cell Biol.* **185**, 11–19 (2009).
11. E. Sahai, Illuminating the metastatic process. *Nat. Rev. Cancer* **7**, 737–749 (2007).
12. D. R. Sherwood, P. W. Sternberg, Anchor cell invasion into the vulval epithelium in *C. elegans*. *Dev. Cell* **5**, 21–31 (2003).
13. D. R. Sherwood, J. A. Butler, J. M. Kramer, P. W. Sternberg, FOS-1 promotes basement-membrane removal during anchor-cell invasion in *C. elegans*. *Cell* **121**, 951–962 (2005).
14. J. W. Ziel, E. J. Hagedorn, A. Audhya, D. R. Sherwood, UNC-6 (netrin) orients the invasive membrane of the anchor cell in *C. elegans*. *Nat. Cell Biol.* **11**, 183–189 (2009).
15. E. J. Hagedorn, H. Yashiro, J. W. Ziel, S. Ihara, Z. Wang, D. R. Sherwood, Integrin acts upstream of netrin signaling to regulate formation of the anchor cell's invasive membrane in *C. elegans*. *Dev. Cell* **17**, 187–198 (2009).
16. B. J. Hwang, A. D. Meruelo, P. W. Sternberg, *C. elegans* EVI1 proto-oncogene, EGL-43, is necessary for Notch-mediated cell fate specification and regulates cell invasion. *Development* **134**, 669–679 (2007).
17. I. Rimann, A. Hajnal, Regulation of anchor cell invasion and uterine cell fates by the egl-43 Evi-1 proto-oncogene in *Caenorhabditis elegans*. *Dev. Biol.* **308**, 187–195 (2007).
18. F. Simmer, C. Moorman, A. M. van der Linden, E. Kuijk, P. V. van den Berghe, R. S. Kamath, A. G. Fraser, J. Ahlinger, R. H. Plasterk, Genome-wide RNAi of *C. elegans* using the hypersensitive *rrf-3* strain reveals novel gene functions. *PLoS Biol.* **1**, E12 (2003).
19. R. S. Kamath, A. G. Fraser, Y. Dong, G. Poulin, R. Durbin, M. Gotta, A. Kanapin, N. Le Bot, S. Moreno, M. Sohrmann, D. P. Welchman, P. Zipperlen, J. Ahlinger, Systematic functional analysis of the *Caenorhabditis elegans* genome using RNAi. *Nature* **421**, 231–237 (2003).
20. J. F. Rual, J. Ceron, J. Koreth, T. Hao, A. S. Nicot, T. Hirozane-Kishikawa, J. Vandenhaute, S. H. Orkin, D. E. Hill, S. van den Heuvel, M. Vidal, Toward improving *Caenorhabditis elegans* phenome mapping with an ORFeome-based RNAi library. *Genome Res.* **14**, 2162–2168 (2004).
21. L. C. McGarry, J. N. Winnie, B. W. O'Zanne, Invasion of v-Fos^{FBR}-transformed cells is dependent upon histone deacetylase activity and suppression of histone deacetylase regulated genes. *Oncogene* **23**, 5284–5292 (2004).
22. T. Zhang, A. Hamza, X. Cao, B. Wang, S. Yu, C. G. Zhan, D. Sun, A novel Hsp90 inhibitor to disrupt Hsp90/Cdc37 complex against pancreatic cancer cells. *Mol. Cancer Ther.* **7**, 162–170 (2008).
23. Y. Naito, T. Yamada, T. Matsumiya, K. Ui-Tei, K. Saigo, S. Morishita, dsCheck: Highly sensitive off-target search software for double-stranded RNA-mediated RNA interference. *Nucleic Acids Res.* **33**, W589–W591 (2005).
24. C. Chang, A. P. Newman, P. W. Sternberg, Reciprocal EGF signaling back to the uterus from the induced *C. elegans* vulva coordinates morphogenesis of epithelia. *Curr. Biol.* **9**, 237–246 (1999).
25. R. D. Burdine, C. S. Branda, M. J. Stern, EGL-17(FGF) expression coordinates the attraction of the migrating sex myoblasts with vulval induction in *C. elegans*. *Development* **125**, 1083–1093 (1998).
26. J. Grantham, K. I. Brackley, K. R. Willison, Substantial CCT activity is required for cell cycle progression and cytoskeletal organization in mammalian cells. *Exp. Cell Res.* **312**, 2309–2324 (2006).
27. X. Zhang, Z. Yuan, Y. Zhang, S. Yong, A. Salas-Burgos, J. Koomen, N. Olashaw, J. T. Parsons, X. J. Yang, S. R. Dent, T. P. Yao, W. S. Lane, E. Seto, HDAC6 modulates cell motility by altering the acetylation level of cortactin. *Mol. Cell* **27**, 197–213 (2007).
28. H. Hasegawa, T. Senga, S. Ito, T. Iwamoto, M. Hamaguchi, A role for AP-1 in matrix metalloproteinase production and invadopodia formation of v-Crk-transformed cells. *Exp. Cell Res.* **315**, 1384–1392 (2009).
29. K. Mitani, Molecular mechanisms of leukemogenesis by AML1/EVI-1. *Oncogene* **23**, 4263–4269 (2004).
30. S. Rodrigues, O. De Wever, E. Bruyneel, R. J. Rooney, C. Gespach, Opposing roles of netrin-1 and the dependence receptor DCC in cancer cell invasion, tumor growth and metastasis. *Oncogene* **26**, 5615–5625 (2007).
31. D. E. White, W. J. Muller, Multifaceted roles of integrins in breast cancer metastasis. *J. Mammary Gland Biol. Neoplasia* **12**, 135–142 (2007).
32. D. C. Drummond, C. O. Noble, D. B. Kirpotin, Z. Guo, G. K. Scott, C. C. Benz, Clinical development of histone deacetylase inhibitors as anticancer agents. *Annu. Rev. Pharmacol. Toxicol.* **45**, 495–528 (2005).
33. P. J. Gray Jr., T. Prince, J. Cheng, M. A. Stevenson, S. K. Calderwood, Targeting the oncogene and kinase chaperone CDC37. *Nat. Rev. Cancer* **8**, 491–495 (2008).
34. I. Ota, X. Y. Li, Y. Hu, S. J. Weiss, Induction of a MT1-MMP and MT2-MMP-dependent basement membrane transmigration program in cancer cells by Snail1. *Proc. Natl. Acad. Sci. U.S.A.* **106**, 20318–20323 (2009).
35. C. E. Rocheleau, J. Yasuda, T. H. Shin, R. Lin, H. Sawa, H. Okano, J. R. Priess, R. J. Davis, C. C. Mello, WRM-1 activates the LIT-1 protein kinase to transduce anterior/posterior polarity signals in *C. elegans*. *Cell* **97**, 717–726 (1999).
36. A. Aouacheria, C. Geourjon, N. Aghajari, V. Navratil, G. Deleage, C. Lethias, J. Y. Exposito, Insights into early extracellular matrix evolution: Spongin short chain collagen-related proteins are homologous to basement membrane type IV collagens and form a novel family widely distributed in invertebrates. *Mol. Biol. Evol.* **23**, 2288–2302 (2006).
37. R. G. Rowe, X. Y. Li, Y. Hu, T. L. Saunders, I. Virtanen, A. Garcia de Herreros, K. F. Becker, S. Ingvarsen, L. H. Engelholm, G. T. Bommer, E. R. Fearon, S. J. Weiss, Mesenchymal cells reactivate Snail1 expression to drive three-dimensional invasion programs. *J. Cell Biol.* **184**, 399–408 (2009).
38. S. Brenner, The genetics of *Caenorhabditis elegans*. *Genetics* **77**, 71–94 (1974).
39. F. Sabeh, I. Ota, K. Holmbeck, H. Birkedal-Hansen, P. Soloway, M. Balbin, C. Lopez-Otin, S. Shapiro, M. Inada, S. Krane, E. Allen, D. Chung, S. J. Weiss, Tumor cell traffic through the extracellular matrix is controlled by the membrane-anchored collagenase MT1-MMP. *J. Cell Biol.* **167**, 769–781 (2004).
40. **Acknowledgments:** We are grateful to P. Sternberg in whose laboratory this study was initiated, E. Cram for *cacn-1(tm3042)* and *cacn-1(tm3082)*, A. Puoti for the *mep-1::GFP* strain, I. Hope for the *F28F8.5::GFP* strain, N. Poulson for the *cdc-37::GFP* strain, F. Mason for *T03F1.8::GFP* strain, A. Hajnal for *egl-43L* primers, C. Hu for help with the CAM assay, J. Ziel for help with statistical analyses, the *Caenorhabditis* Genetics Center for providing additional strains, and E. Hagedorn, M. Yang, J. Ziel, N. Matus, and D. Killebrew for comments on the manuscript. **Funding:** D.Q.M. is a Robert Black Fellow of the Damon Runyon Cancer Research Foundation (DRG-1949-07). This work was supported by NIH grants CA088308 and CA116516 and the Breast Cancer Research Foundation (to S.J.W.) and a Basil O'Connor Award, Pew Scholars Award and NIH grants GM079320 and K01 CA098316-01 (to D.R.S.). **Author contributions:** D.Q.M., S.D., S.J.W., and D.R.S. participated in the experimental design; D.Q.M., X.-Y.L., S.D., D.A., Q.C., and D.R.S. participated in data acquisition and analysis; D.Q.M., S.J.W., and D.R.S. wrote the manuscript.

Submitted 18 September 2009

Accepted 16 April 2010

Final Publication 4 May 2010

10.1126/scisignal.2000654

Citation: D. Q. Matus, X.-Y. Li, S. Durbin, D. Agarwal, Q. Chi, S. J. Weiss, D. R. Sherwood, In vivo identification of regulators of cell invasion across basement membranes. *Sci. Signal.* **3**, ra35 (2010).